



## Sustainable approaches in textile dyeing sludge management: A review of emerging technologies and future perspective

Raju Lavanya & Dhanapal Vasanth Kumar \*

VIT Fashion Institute of Technology, Vellore Institute of Technology, Chennai, Tamil Nadu, India

\*E-mail: vasanthkumar.d@vit.ac.in / cuteevasanth@gmail.com

*Received 11 July 2025; accepted 24 February 2026*

The textile dyeing sector produces a significant amount of sludge from Effluent Treatment Plants (ETPs), leading to serious environmental issues due to ineffective traditional disposal practices. This research reviews the sustainable approaches for the sludge management of bio, salt, and lime sludge generated during effluent treatment. A detailed characterization of all the sludges was done using CHNS, TGA-DTA-DTG, ICP-MS, SEM-EDS, XRD, and FTIR analysis. Bio-sludge showed high carbon, 25.86%, in comparison to other sludges. The salt-sludge showed significant levels of sulfur 5.45% and sodium, 21.95 wt.%, whereas the lime-sludge was alkaline in nature with pH 10.02 and increased calcium levels, 22.2wt.%. The ICP-MS results showed that salt-sludge contained high levels of heavy metals, particularly Cu (1038.44 ppm), Zn (103.10 ppm), and Hg (284.30 ppb), which highlights issues related to potential toxicity. The TGA exhibited multi-stage decomposition for all samples, with considerable weight loss recorded in bio-sludge, consistent with its volatile content. SEM-EDS showed porous carbonaceous structures in bio-sludge, in contrast to the crystalline salt clusters in salt-sludge and layered mineral formations in lime-sludge. These results establish bio-sludge as a promising option for pyrolytic conversion due to its rich organic content and energy potential. Although salt sludge has a lower organic fraction, it is suitable for controlled gasification if heavy metals are carefully monitored. Lime-sludge, with its inorganic stability and low moisture content, can act as a co-feed in thermal processes or co-processing in cement manufacturing. Hence, the sludges demand customized treatment strategies to transform them into energy, biochar, or industrial raw materials, fostering the principles of a circular economy and reduced environmental impacts.

**Keywords:** Biological remediation, Cement replacement, Circular economy, Textile effluent sludge, Thermochemical remediation

### Introduction

The textile and apparel sector in India is presently experiencing significant expansion, stimulated by multifaceted policy initiatives, market dynamics, and other international factors. The Indian government has framed an ambitious agenda for the textile sector, aiming for a 20% share in the global textile market and a domestic industry valued at \$650 billion by the fiscal year 2024-25<sup>1</sup>. The sector is experiencing structural changes to align with the demands of global buyers, who stress the significance of sustainable practices<sup>2</sup>. Tirupur, known as India's knitwear capital, is a major export hub renowned for its extensive production of premium cotton garments, particularly hosiery, pullouts, towels, napkins, and knitwear, significantly impacting the export of the sector by accounting for almost 90% of the nation's cotton knitwear exports globally.

The hub has approximately 760 dyeing units, of which around 430 units are currently operational,

supporting the region's textile production and export infrastructure<sup>3</sup>. The rising concerns related to the governance of Textile dyeing effluent and Sludge (TS), generated as an undesirable byproduct of the process, have prompted the need for innovative treatment technologies. Under these circumstances, Common Effluent Treatment Plants (CETPs) or Individual Effluent Treatment Plants (IETPs) were integrated into the system to drain treated wastewater into the local river Noyyal, which was managed by the Tamil Nadu Pollution Control Board (TNPCB). Further, in 2006, a crucial legal mandate was instituted, convincing all dyeing units to adopt Zero Liquid Discharge (ZLD) systems, thereby strictly prohibiting the direct release of any effluent into the river. To adhere to this regulation, industries commissioned ZLD systems in all their facilities by 2010, which incorporated Reverse Osmosis (RO) systems together with reject management systems. There are 19 CETPs with a combined treatment

capacity of 1,02,250 KLD (kilolitres per day). The consortium has over 455 total members, out of which 370 are actively participating in the effluent treatment process, reflecting a strong but slightly varied commitment to environmental management in textile industry of Tirupur<sup>4</sup>.

Each CETP serves anywhere between 4 to 75 member units and the daily generated effluent is gathered for centralized treatment. The effluent is first directed to the equalization tank to ensure consistent mixing, followed by its transfer to the aeration tank for anaerobic biological treatment. After this stage, the biologically treated effluent is directed to the secondary clarifier, where organic impurities are transformed into bio-sludge, and the clarified effluent is sent for additional processing. The secondary-treated effluent then receives advanced treatment at the Reverse Osmosis (RO) plant. Upon completion of the 5 RO stages, the effluent is moved to the clariflocculator, where chemical additives like lime and lye are added to promote precipitation. The resulting slurry is dewatered to form the lime-sludge, and the brine solution generated as permeate from the RO process is reclaimed and distributed among member units for reuse, contributing to water conservation efforts<sup>5</sup>.

At the same time, the RO reject is processed further using Multiple Effect Evaporators (MEE) or Mechanical Vapour Re-compressors (MVR), enabling the recovery of extra water. At this stage, approximately 90% of the effluent received by the

plant is treated and reutilized by member units. The concentrated brine solution is subjected to centrifugation and crystallization, facilitating the recovery of reusable salt. The liquid separated during centrifugation is directed to solar evaporation pans, resulting in the formation of salt-sludge. The salt sludge is collected and securely disposed of in a designated landfill facility, ensuring environmentally sound waste management practices<sup>4</sup>.

Fig. 1 illustrates a typical flow of effluent treatment in a CETP in Tirupur. Untreated effluent contains hydrolyzed dyes that threaten aquatic ecosystems by compromising water clarity, interfering with photosynthesis, reducing dissolved oxygen levels, and negatively impacting marine species<sup>7</sup>. Many dyes, particularly azo dyes, resist oxidation, aerobic degradation, and physical separation, posing risks of bioaccumulation and biomagnification in the food chain. Due to their refractory nature, dye compounds tend to accumulate in biomass<sup>8</sup>. Hence, managing sludge effectively in textile wastewater treatment is vital for preventing environmental contamination and addressing the dangers related to hazardous chemicals, like heavy metals and dyes, which may permeate into the ecosystems. TS remediation requires a decision-oriented approach, as technology selection is governed primarily by sludge composition, inorganic load, and process compatibility rather than treatment efficiency alone. Sludge produced by CETPs is categorized into bio-sludge, salt-sludge, and lime-

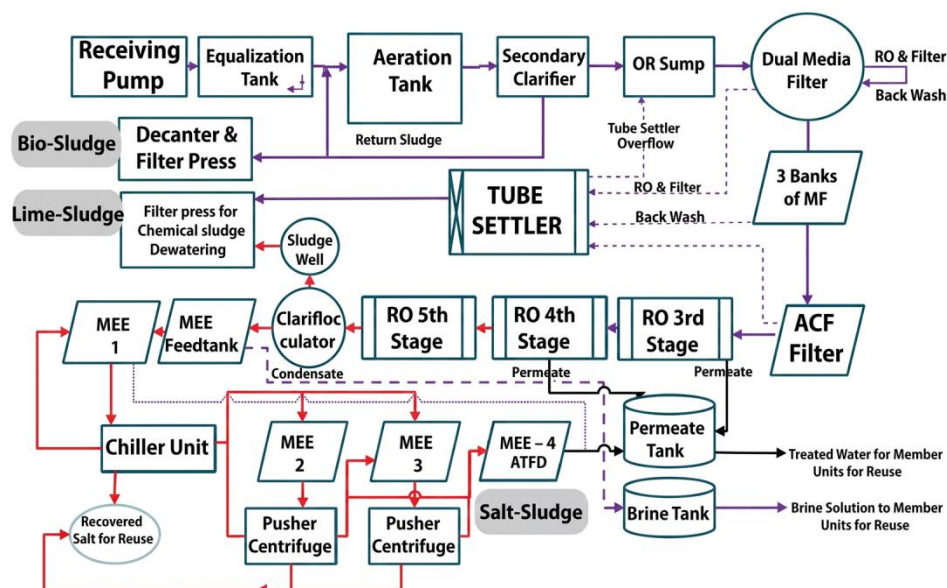


Fig. 1 — Process Flow diagram of CETP<sup>6</sup>

sludge. Each variant has unique physicochemical properties that distinctly influence reactor performance, energy recovery efficiency, corrosion rates, and the quality of the by-product. Accordingly, this review classifies remediation pathways into energy and material or resource recovery-oriented technologies, explicitly mapping each sludge type to suitable options based on process design, operating conditions, scale-up feasibility, techno-economic constraints, and sustainability considerations. In this study, we explored the characteristics of the sludges and assess available remediation techniques through a comprehensive literature survey, emphasizing the need for sustainable practices to protect the environment and ensure regulatory compliance.

#### Characterization of TS

The sludge samples used in this study were collected from one of the fully functional CETPs in Tirupur. The particular CETP was designated for sample collection because of its proximity to the residential part of the city to analyze and characterize the hazardous nature of the sludge and assess its impact on the environment. All 3 sludges, namely bio, lime, and salt-sludge procured, were drained off their water and sundried for several weeks in the plant, and the resulting products are as shown in Fig. 2. The physicochemical characterization and recovery potential of the sludges generated from the treatment of textile wastewater are imperative to provide insights into their composition and possible valorization options.

#### Physicochemical characteristics

Table 1 illustrates a comparative study of bio-sludge, salt-sludge, and lime-sludge, emphasizing their elemental characteristics, pH measurements, moisture content, conductivity, resistivity, and levels of important nutrients, including phosphate and nitrate. Bio-Sludge demonstrates an exceptional organic composition, with carbon (25.86%), nitrogen (4.26%), and hydrogen (7.75%), emphasizing its strong biological origin. Its elevated moisture content (43%) and high conductivity (1352  $\mu\text{S}/\text{cm}$ ) indicate a substantial presence of dissolved ions, rendering it highly suitable for organic applications, including composting and bio-fertilization. Furthermore, its nitrate concentration (20.41 mg/L) and phosphate levels (3.05 mg/L) significantly exceed those observed in other sludge varieties, emphasizing its rich nutrient profile. The salt-sludge is characterized by a significant sulfur content of 5.45% while



Fig. 2 — (a) Bio-sludge, (b) lime-sludge and (c) salt-sludge

Table 1 — Physico-chemical characteristics of bio, salt, and lime-sludge

Sludge Type	Bio-sludge	Salt-sludge	Lime-sludge
Parameters			
N%	4.26	0.17	Not Detected
C%	25.86	0.95	9.09
S%	1.72	5.45	0.99
H%	7.75	0.36	0.51
pH	8.44	7.95	10.02
Moisture %	43.00	14.8	5.09
Conductivity( $\mu\text{S}/\text{cm}$ )	1352	13.06	3.210
Resistivity (k $\Omega/\text{cm}$ )	0.741	0.078	0.314
Phosphate (mg/L)	3.050	0.310	1.860
Nitrate (mg/L)	20.410	8.730	8.730

exhibiting minimal organic components (carbon: 0.95%, nitrogen: 0.17%), clearly indicating an inorganic composition. The values of conductivity at 13.06  $\mu\text{S}/\text{cm}$  and resistivity at 0.078 k $\Omega/\text{cm}$  suggest a limited concentration of dissolved ions. The moderately neutral pH of 7.95 and reduced moisture content of 14.8% are consistent with its predominantly mineral-based nature. The relatively low levels of phosphate (0.31 mg/L) and nitrate (8.73 mg/L) further suggest that salt-sludge possesses minimal fertility value. Lime-sludge is distinguished by its pronounced alkalinity of pH 10.02 and moderate carbon content of 9.09%, indicating its potential utility as a neutralizing agent in both industrial and agricultural applications. Its negligible nitrogen and sulfur content (0.99%), combined with low moisture levels (5.09%), set it apart from the other sludge types. The extremely low conductivity (3.21  $\mu\text{S}/\text{cm}$ ) and moderate resistivity (0.314 K $\Omega/\text{cm}$ ) imply a less soluble composition. Despite phosphate levels (1.86 mg/L) and nitrate levels (8.73 mg/L) being higher than those in salt-sludge, they are still lower than those in bio-sludge when compared.

The notable differences in organic content, salinity, and alkalinity availability among the three TS types strongly influence their remediation and valorization potential. The high carbon, nitrogen, and moisture

content of bio-sludge favours biological conversion and thermochemical energy recovery routes<sup>9</sup>, whereas the low organic fraction and high mineral content of salt- and lime-sludge constrain biodegradation and limit their suitability for energy-oriented processes<sup>10</sup>. Inorganic sludges prove to be excellent for stabilization, retrieving minerals, or in various applications that concentrate on neutralization.

#### Trace and heavy metal analysis

The Inductively Coupled Plasma Mass Spectrometry (ICP-MS) was used with a Thermo Fisher iCAP RQ ICP-MS instrument, to understand the elemental composition of lime, salt, and bio-sludge, especially concerning trace and heavy metal elements. Lime sludge demonstrates high levels of aluminum (116.75), barium (70.10), and boron (65.06), which indicates the existence of mineral-derived compounds. The calcium level (2.3) suggests a lime origin, while the moderate concentrations of lead (2.83), chromium (4.81), and nickel (7.20) indicate the potential for trace metal pollution. The minimal amounts of arsenic (1.49) and selenium (0.27) indicate limited contamination from toxic metals. Salt sludge reveals significantly raised sodium levels (31.5), which correspond to its saline characteristics. The high concentrations of antimony (120.99), boron (16.82), and moderate zinc (6.58) confirm its industrial origin. However, it registers molybdenum and leads under the detection limit, making it relatively less polluted with heavy metals compared to the other samples.

Bio sludge is abundant in heavy metals, showcasing particularly high levels of aluminum (714.97), copper (1083.44), and zinc (1031.05). Additionally, the iron content (5.0) exceeds that of the other samples, suggesting the presence of biological

or organic matter that has accumulated metals. The high concentrations of lead (3.97), chromium (15.29), and nickel (11.47) increase concerns regarding potential toxicity. Moreover, the elevated mercury levels (284.30) render it inappropriate for certain uses without adequate treatment. Fig. 3 illustrates a heatmap representation of metals with higher concentration appearing in red and those with lower concentration appearing in blue and yellow. The high levels of heavy metal concentration found in Bio-sludge (Cu, Zn, Cr, Hg) have a direct implication on disposing of TS in landfills and require controlled remediation pathways. But these metals can be immobilized during thermochemical treatments by means of char encapsulation or ash vitrification, making thermal routes more appropriate than biological reuse<sup>11</sup>.

#### Thermogravimetric analysis (TGA) analysis

TGA-DTA Hitachi STA7000 and DSC Netzsch 204 F1 Heat flux DSC was used to analyze the thermal stability, decomposition mechanisms, and inorganic content of the samples. This comparative investigation can enhance the understanding of the thermal properties and potential practical applications of each material, encompassing aspects such as energy potential, the efficiency of lime calcination, and the purity of salt.

The TGA of the bio sample reveals multiple stages of mass loss, suggesting a complex process of organic decomposition. The reduction in mass was observed in the range 50–150°C, which is a characteristic of biomass materials containing inherent moisture. A prominent degradation stage is distinguished in the temperatures of 200–500°C, which relates to the thermal disintegration of hemicellulose, cellulose, and lignin. This specific temperature range is indicative of

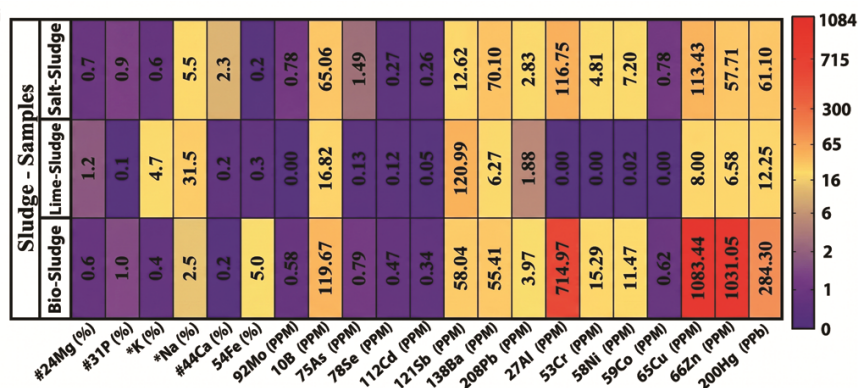


Fig. 3 — Heatmap of elemental composition of bio, lime, and salt sludge

the combustion of volatile compounds alongside organic matter. Above 500°C, the mass remains relatively stable, exhibiting only minor degradation, which is likely a consequence of the oxidation of char residues, as can be inferred from Fig. 4a. The residual mass may predominantly comprise ash content derived from the inorganic minerals present within the bio sample. The TGA profile of the lime sample is distinguished by a reduced number of degradation steps. A minor initial weight reduction observed below 150°C suggests the desorption of absorbed moisture. A notable decrease in mass seems to occur within the temperature range of 600-800°C, linked to the conversion of calcium carbonate ( $\text{CaCO}_3$ ) into calcium oxide ( $\text{CaO}$ ) along with the release of carbon dioxide. Beyond this temperature, the sample exhibits thermal stability, with minimal mass loss, indicating the formation of stable  $\text{CaO}$ , as shown in Fig. 4b. The TGA behaviour of the salt sample reveals a more straightforward pattern of thermal decomposition. The initial weight loss observed up to 150°C may be due to the evaporation of residual or hydrated water contained within the salt crystals. A minor mass loss occurring around 250–350°C may be attributed to the decomposition of trace impurities or volatile

contaminants, as evident in Fig. 4c. The primary thermal stability observed above 400°C suggests the non-volatile characteristics of the salt, indicating a minimal presence of organic content and a high residual mass.

The DTG (Derivative Thermogravimetry) and DTA (Differential Thermal Analysis) of salt, lime, and bio sludge samples reveal distinct thermal degradation patterns associated with their composition. The salt-sludge exhibits decomposition stages, with a major reaction around 900°C attributed to the salt melting and another secondary reaction around 1100°C showing solidification or recrystallization. The lime-sludge displays a dual thermal degradation mechanism, where the initial endothermic peak occurring at 400-500°C indicates dehydration. A strong peak around 800-900°C exhibits an endothermic reaction caused by the breakdown of  $\text{CaCO}_3$ . A minor endothermic reaction at 900-1200°C may be due to the possible formation of calcium silicate. The bio-sludge exhibits minor endothermic reactions between 50-150°C and 200-500°C due to moisture loss and organic matter decomposition. A significant exothermic peak between 500-700°C indicates combustion of residual

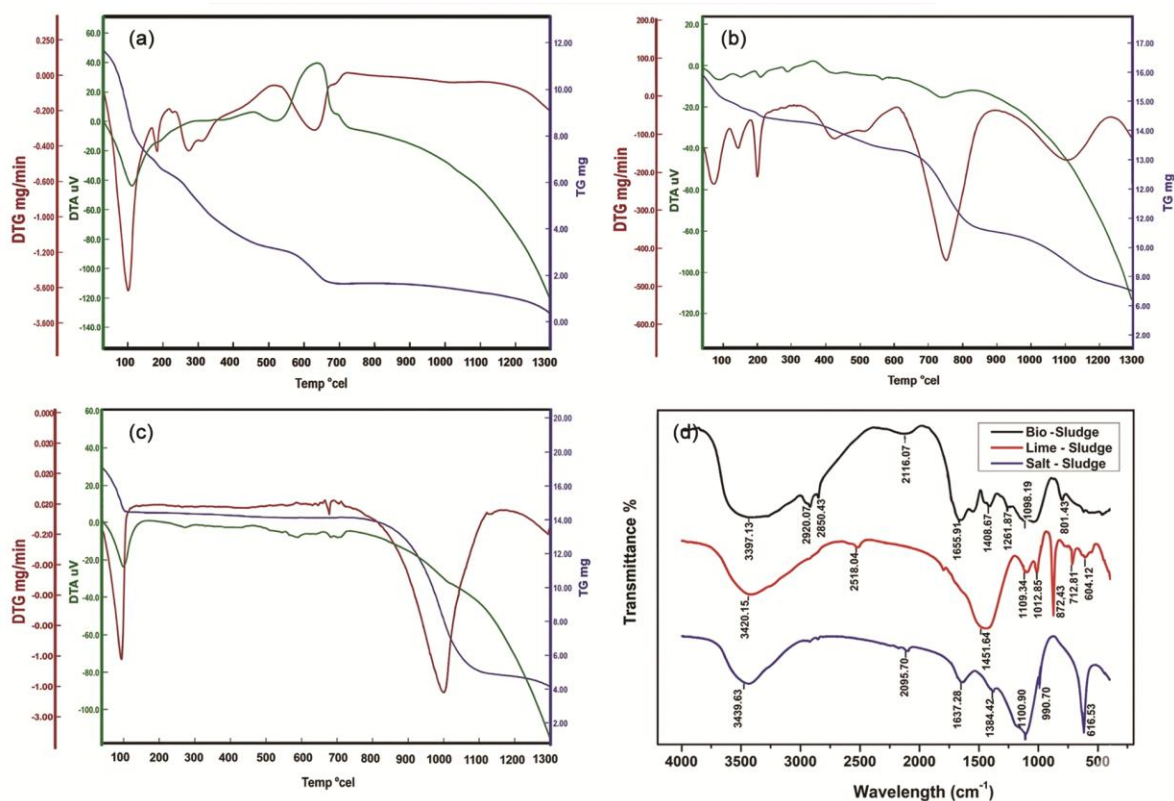


Fig. 4 — (a) TGA, (b) DTA, (c) DTG and (d) FTIR spectra of bio-sludge, lime-sludge, and salt-sludge

carbon. The DTG curves confirm the faster degradation of bio-sludge, while DTA peaks highlight exothermic oxidation of organics in bio samples, endothermic carbonate decomposition in lime-sludge, and endothermic salt melting and crystallization in salt-sludge.

Thermal degradation behaviour observed through TGA, DTG, and DTA analysis influences the TS process selection. The multi-stage organic decomposition and high volatile release of bio-sludge between 200–500°C demonstrate its compatibility with pyrolysis and gasification, whereas the thermal stability and mineral dominance of salt and lime-sludge above 400°C decisively render them inappropriate for syngas production but highly advantageous for mineral transformation and stabilization processes<sup>12</sup>.

#### Fourier Transform Infrared Spectroscopy (FTIR) of TS

Thermo Nicolet iS50 FTIR spectrometer 4000  $\text{cm}^{-1}$  to 100 $\text{cm}^{-1}$ , with a resolution of 0.2  $\text{cm}^{-1}$ , was used to analyze the samples, and the spectrum thus obtained is represented in Fig. 4d. The broad peak of the Bio-Sludge observed at 3397  $\text{cm}^{-1}$  signifies O-H stretching, which is linked to hydroxyl (-OH) groups or water molecules. The peaks at 2920 and 2850  $\text{cm}^{-1}$  correspond to C-H stretching, typically found in aliphatic hydrocarbons. A weaker peak at 2116  $\text{cm}^{-1}$  may be attributed to  $\text{C}\equiv\text{C}$  or  $\text{C}\equiv\text{N}$  stretching, indicating the presence of alkyne or nitrile groups. The peak at 1655  $\text{cm}^{-1}$  indicates C=O stretching (carbonyl), originating from amides or carboxyl groups. The spectral range of 1408-1261  $\text{cm}^{-1}$  may imply the occurrence of C-H bending or C-O stretching vibrations. Furthermore, the spectral interval of 1098-801  $\text{cm}^{-1}$  indicates C-O stretching or Si-O-Si bond characteristics. The presence of C-H groups, C=O components, and hydroxyl groups indicates an abundance of natural compounds in the sample. This sample demonstrates a composition that includes cellulose, lignin, and fatty acids, along with the presence of silicates and minerals, which could be attributed to contamination from soil or sediment sources.

The extensive peak observed at 3420  $\text{cm}^{-1}$  in lime-sludge suggests O-H stretching, associated with hydroxyl groups. The peak recorded at 2518  $\text{cm}^{-1}$  indicates the presence of carbonate species of  $\text{CaCO}_3$ . The peaks at 1451 and 1384  $\text{cm}^{-1}$  are indicative of carbonate stretching vibrations, thereby corroborating the existence of  $\text{CaCO}_3$ . The spectral range of 1109-604  $\text{cm}^{-1}$  is associated with metal-oxygen bond

interactions and Si-O vibrational modes. It exhibits a lower organic content in comparison to bio-sludge. The observed increase in mineral and carbonate species suggests that the stabilization of sludge may arise from the incorporation of lime or related chemicals.

The broad peak of salt sludge observed at 3439  $\text{cm}^{-1}$  signifies O-H stretching, related to hydroxyl groups or water. The peak at 2095  $\text{cm}^{-1}$  may be associated with  $\text{C}\equiv\text{C}$  or  $\text{C}\equiv\text{N}$  stretching. The peaks at 1637 and 1384  $\text{cm}^{-1}$  suggest the presence of carboxylate or carbonate groups. The range of 1100-616  $\text{cm}^{-1}$  is associated with Si-O and metal-oxygen vibrations. Salt-sludge demonstrates a strong mineral influence, particularly from silicates and carbonates. While it retains some organic components, structural alterations due to interactions with salt are evident. The presence of nitrile ( $-\text{C}\equiv\text{N}$ ) implies protein degradation, potentially linked to changes in microbial activity under saline conditions. Salt-Sludge displays inorganic signatures, suggesting possible interactions between salt and sludge components.

The presence of hydroxyl (-OH) groups is evident in all samples, as they exhibit a broad peak around 3400  $\text{cm}^{-1}$ . The peaks indicating  $\text{CaCO}_3$  are most pronounced in lime-sludge at 2518  $\text{cm}^{-1}$  and 1451  $\text{cm}^{-1}$ , confirming the presence of calcium carbonate. The aliphatic C-H stretching observed at 2920  $\text{cm}^{-1}$  is present in bio-sludge but absent in the other two, suggesting a higher organic content in bio-sludge. Both salt-sludge and lime-sludge display more intense peaks in the lower wavenumber region (1000-600  $\text{cm}^{-1}$ ) for Si-O and metal-oxygen bonds, indicating a greater presence of inorganic components. The nitrile/alkyne stretching observed at 2100  $\text{cm}^{-1}$  is present in bio-sludge and salt-sludge but is missing from lime-sludge.

FTIR analysis further substantiates the differentiation in technology, as the high presence of oxygenated functional groups (-OH, C=O, C-H) in bio-sludge improves both biodegradability and thermochemical reactivity. Conversely, the prevalence of carbonate, silicate, and metal-oxygen bonds in salt and lime-sludge restricts biological conversion and promotes inorganic valorization or immobilization approaches<sup>9</sup>.

#### Scanning Electron Microscope and Energy Dispersive X-ray Spectroscopy

The surface morphology of the samples was investigated using Scanning Electron Microscopy

(SEM) (JEOL JSM-6390), which was operated at an accelerating voltage of 20 kV utilizing a Secondary Electron Imaging (SEI) mode. The images were collected at a magnification level of 7000x, maintaining a working distance of 13 mm. The SEM analysis of bio-sludge indicates an assembly of aggregated or porous particles exhibiting rough textures, which could denote a biological origin (including bacteria, biofilm, or organic materials with mineral inclusions) as represented in Fig. 5a. The elements detected by Energy Dispersive X-ray Spectroscopy (EDX) in bio sludge include C, O, Na, Si, S, P, Cl, Mg, Al, K, and Ca, as shown in Fig. 5 (b). The pronounced peaks in EDX corresponding to Carbon and Oxygen imply that the specimen is predominantly organic in nature, potentially of biological origin, or comprising organic matter interspersed with mineral constituents. Additional elements such as Sodium, Silicon, Sulfur, and Calcium may signify the presence of biominerals, salts, or other compounds. The detection of elements

such as Calcium, Phosphorus, and Sulfur may suggest the existence of biogenic materials, biofilm, or biomineralized tissues.

The SEM analysis of lime-sludge shows certain areas with rod-like or needle-like formations, which may signify specific crystalline structures of calcium-based compounds. The structure indicates a mineral-based compound. The rough, clustered morphology, as denoted in Fig. 5c, is characteristic of precipitated calcium minerals or lime particles. The primary components identified are Ca, O, C, Mg, Na, Si, P, S, Cl, and K, as shown in Fig. 5d.

The substantial presence of calcium strongly affirms that the sample is saturated with materials associated with calcium, very likely comprising  $\text{CaCO}_3$  or calcium hydroxide,  $\text{Ca}(\text{OH})_2$ . The existence of oxygen and carbon reinforces the likelihood of  $\text{CaCO}_3$  being a significant constituent. Additional elements such as magnesium, sodium, and silicon may suggest the presence of minor mineral impurities. The combination of higher calcium levels and a

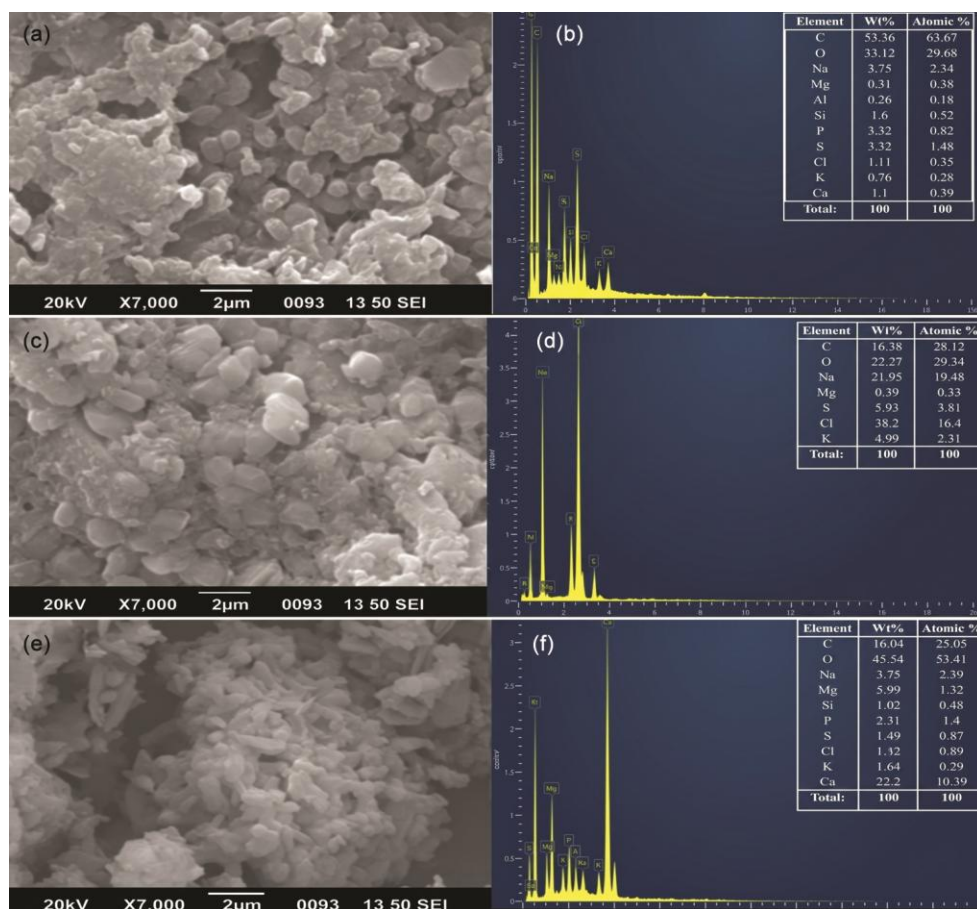


Fig. 5 — (a) SEM and (b) EDX composition of bio-sludge, (c) SEM and (d) EDX composition of lime-sludge, (e) SEM and (f) EDX composition of salt-sludge

crystalline porous structure strongly indicates that this sample could be lime ( $\text{CaO}/\text{Ca}(\text{OH})_2$ ) or calcium carbonate ( $\text{CaCO}_3$ ). As the sludge is a by-product of industrial effluent treatment, it could likely be hydrated lime ( $\text{Ca}(\text{OH})_2$ ) or quicklime ( $\text{CaO}$ ).

The SEM of salt-sludge shows significant sodium and chlorine, confirming that the sample is likely composed of sodium chloride ( $\text{NaCl}$ ), and the crystalline characteristics imply that the substance may represent sea salt or a composite of various salts rather than pure table salt, as can be seen in Fig. 5e. The presence of magnesium, potassium, and sulfur implies there may be contaminants or other mineral structures, including magnesium sulfate ( $\text{MgSO}_4$ ) or potassium chloride ( $\text{KCl}$ ), which is apparent in Fig. 5f. The SEM and EDX show that the sample largely comprises salt-derived material, yet it also shows a small quantity of contaminants.

The lime sludge exhibits non-uniform, porous, and agglomerated particle morphology, revealing a heterogeneous distribution of both fine and coarse granules. Its surface texture is marked by roughness, porosity, and aggregation, which significantly contribute to its unique physical attributes. In contrast, the salt sample is distinguished by a well-structured crystalline arrangement, displaying uniform angular granules, in addition to a smooth surface adorned with sharp-edged crystals that reflect its intrinsic crystalline characteristics. The biological sample, conversely, reveals a fibrous, porous, and cellular-like structure, characterized by irregularly shaped particles that may exhibit either elongated or rounded configurations. Its surface texture is soft, organic, and demonstrates high porosity, which serves as an indicator of its biological origin. The porous, heterogeneous morphology of bio-sludge promotes mass transfer and reaction kinetics in both biological and thermal systems, whereas the dense crystalline structure of salt and lime-sludge restricts microbial accessibility and volatile release, limiting their performance in energy recovery processes<sup>13</sup>.

#### Powder X-ray diffraction (PXRD) analysis

The PXRD assessment in the Bruker D8 advance instrument was conducted applying a  $\text{Cu K}\alpha$  radiation source ( $\lambda = 1.5406 \text{ \AA}$ ) operating at 40 kV and 35 mA, using a coupled Two Theta/Theta scanning at ambient temperature. The PXRD spectrum of bio, lime, and salt-sludge is represented in Fig. 6. The PXRD analysis of the bio-sludge sample reveals mineral phases typically linked to biological and

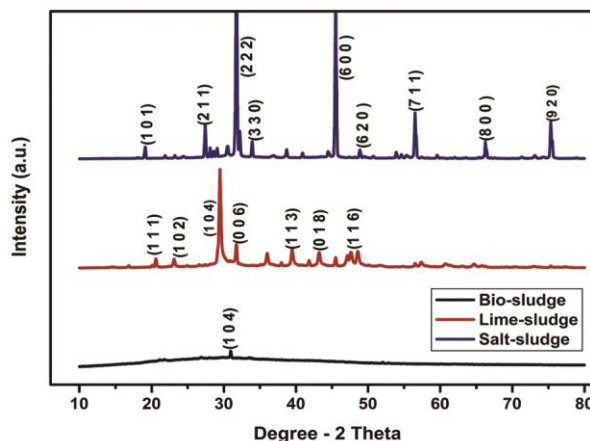


Fig. 6 — PXRD of bio, lime, and sludge samples

environmental substances. The primary phase detected is Hydroxyapatite ( $\text{Ca}_{10}(\text{PO}_4)_6(\text{OH})_2$ ) (JCPDS PDF#: 09-0432), characterized by a prominent peak at  $30.9^\circ$ , signifying its existence, likely from biological activities. Calcium phosphate phases, including  $\beta$ -tricalcium phosphate ( $\beta$ -TCP) and dicalcium phosphate dihydrate (DCPD) (JCPDS PDF#: 09-0169), were identified as secondary constituents. The diffraction peaks between  $21$ – $35^\circ$  indicate the presence of by-products from biomineralization. A small peak at  $26.8^\circ$  suggests the potential existence of silicon dioxide ( $\text{SiO}_2$ , Quartz) (JCPDS PDF#: 46-1045), which could originate from environmental contamination or composite materials. Another minor peak around  $29.9^\circ$  aligns with calcium carbonate ( $\text{CaCO}_3$ , Calcite) (JCPDS PDF#: 05-0586), frequently found in natural biomaterials.

The analysis of the lime-sludge specimen shows two major crystalline phases. The dominant phase is calcite ( $\text{CaCO}_3$ ), with 69.7% (PDF 01-071-3699), and is classified within the rhombohedral crystal system. This shows that a substantial portion of the Lime-sludge is constituted of  $\text{CaCO}_3$  in its stable crystalline configuration. The second phase identified is monohydrocalcite ( $\text{CaCO}_3 \cdot \text{H}_2\text{O}$ ) of 30.3% (PDF 01-076-7969), which crystallizes within the hexagonal crystal system. It is the hydrated variant of  $\text{CaCO}_3$ , presumably arising from the partial hydration of calcite under aqueous conditions or during the synthesis of lime-sludge. The analysis of the salt-sludge sample confirms the presence of crystalline salt phases. The predominantly identified phases consist of sodium chloride ( $\text{NaCl}$ ) (JCPDS No. 05-0628), noted for a pronounced diffraction peak at around  $31.7^\circ$ , which signifies the presence of table

salt. The notable peaks appearing at roughly 31.9° and 22.0° suggest that sodium sulfate (Na<sub>2</sub>SO<sub>4</sub>) (JCPDS No. 19-1454) has formed as a result of chemical additives or contaminants. The XRD findings reveal that the salt-sludge is mainly made up of sodium-based salts. PXRD results confirm that bio-sludge contains biologically derived calcium phosphates and mixed mineral phases that can undergo thermochemical transformation, while the dominance of stable crystalline CaCO<sub>3</sub> and NaCl phases in lime and Salt-sludge explains their poor reactivity during thermal conversion and reinforces their unsuitability for syngas-oriented technologies<sup>11</sup>.

#### **Implications of TS properties on remediation and valorization pathway selection**

The characterization of TS definitively establishes that remediation and valorization pathways must be tailored to specific sludge types rather than being broadly applied. Bio-sludge, defined by its high organic content, moisture, volatile matter, and reactive functional groups, is suited for biological treatment, pyrolysis, and gasification-based energy recovery. In contrast, salt-sludge and lime-sludge possess low organic fractions, high mineral stability, and limited thermal reactivity, making them entirely inappropriate for syngas generation, yet perfectly suited for stabilization, neutralization, or mineral recovery strategies. These findings clearly provide a property-driven foundation for the technology prioritization outlined in the following sections.

#### **Thermo-chemical treatments**

The management of sludge resulting from textile effluent treatment has escalated into a vital ecological concern because it can pollute soil, water, and air<sup>14</sup>. Various disposal techniques have been developed, ranging from conventional methods like incineration and landfilling to advanced approaches such as vermi-stabilization, wet oxidation, and thermochemical methods like pyrolysis, gasification, and liquefaction that offer sustainable alternatives with recovery efficiencies<sup>15</sup>.

A range of thermo-chemical processes is available for managing waste, including methods like wet oxidation, liquefaction, and pyrolysis. These techniques are crucial in transforming organic waste into valuable by-products. When feedstocks with elevated moisture, like TS is used, drying becomes an essential pre-treatment procedure<sup>9</sup>. Among the different methods, pyrolysis and liquefaction are widely used to convert organic substances into bio-

oil (crude), which could function as a plausible renewable energy replacement. However, gasification generates syngas, a fusion of hydrogen, carbon monoxide, and assorted gases, which can then be enhanced into energy or chemicals<sup>16</sup>. The upcoming section will outline a few thermochemical approaches used to treat TS.

#### **Gasification**

Gasification has been investigated as an energy recovery route for TS due to its ability to convert hazardous waste into syngas while achieving significant volume reduction. However, the technical feasibility of gasification is strongly dependent on TS composition. Hydrothermal gasification enables direct processing of high moisture TS at 300-600°C and 20-42.5 MPa, eliminating the need for drying and achieving carbon gasification efficiencies up to 86% with hydrogen-rich syngas, particularly in the presence of alkaline catalysts such as KOH<sup>9,16</sup>. Despite high conversion efficiency, the requirement for high-pressure reactors and susceptibility to salt-induced corrosion are constraints for scale-up and industrial deployment for TS.

Co-gasification combined with hydrothermal carbonization converts TS into reactive hydrochar at 180-220°C, followed by gasification with coal at elevated temperatures, enhancing syngas yield and fuel flexibility<sup>17</sup>. Nevertheless, the multi-step nature of the process, dependence on co-feeding, and increased system complexity limit its applicability as a standalone TS valorization route. Supercritical water gasification (SCWG) operates above 374°C and 22 MPa, where water acts as both a solvent for supercritical water gasification operates above 374°C and 22 MPa, producing hydrogen and methane rich gas with conversion efficiencies approaching 70%<sup>18</sup>. While effective for wet TS, extreme operating conditions, catalyst instability in salt-rich matrices and high capital requirements significantly restrict its industrial feasibility.

Microwave-assisted systems enable rapid and uniform heating of TS, achieving improved energy and exergy efficiencies at optimized temperatures (approx. 450°C)<sup>19</sup>. Scale-up remains limited by microwave penetration depth, sludge heterogeneity, and high electrical energy demand. A comparative evaluation of gasification technologies, operating conditions, and performance implications is provided in Table 2, while the generalized process configuration is shown in Fig. 7.

Table 2 — Comparative review of different Gasification methods

Method	Process Parameters	Key Findings	TS Suitability and constraint	Ref.
Hydrothermal Gasification	300–600°C, 10–30 MPa, Water as medium	High carbon conversion efficiency (up to 86%) with significant hydrogen yield.	Suitable for wet bio-sludge; salt-induced corrosion/scaling limits Salt-sludge; unsuitable for Lime-sludge	[9,16]
Co-Gasification	700–1000°C Oxygen or Steam, Mixed feedstock	Enhances the reactivity of hydrochar with coal, improving syngas production.	Conditionally suitable for bio-sludge; requires co-feeding; limited self-sustained TS applicability	[17]
Supercritical Water	>374°C, >22 MPa, Water as medium	Achieves 70% conversion into gas/liquid, with high calorific value gas.	Effective for wet bio-sludge; extreme pressure, salt fouling, and high cost restrict TS scale-up	[18]
Pyrolysis-Gasification	500–900°C, Inert or oxidative environment	Flexible processing with co-pyrolysis, producing bio-oil, biochar, and syngas.	Suitable for bio-sludge; high ash/salt content reduces syngas quality and reactor stability	[55,56]
Microwave-Assisted	450°C, Microwave frequency heating	Optimized at 450°C for energy efficiency, with rapid heating and uniformity.	Laboratory-scale promising; scale-up limited by microwave penetration and energy demand	[19]
Integrated Systems	Varies based on process combination	Compact design with high energy recovery and waste reduction.	Best for bio-sludge; salt fouling degrades syngas quality and operational stability	[57]

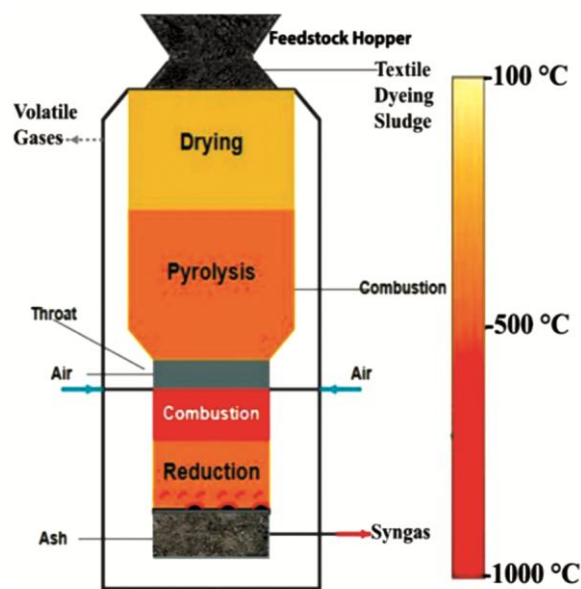


Fig. 7 — Schematics of a TS gasification process

### Pyrolysis

Pyrolysis stands as a powerful thermochemical method for the valorization of TS, effectively converting it into biochar, bio-oil, and syngas under oxygen-free conditions. When compared to incineration, pyrolysis ensures emissions and product quality, while also enhancing energy and material recovery. The schematics of a typical pyrolysis process are represented in Fig. 8. Microwave-assisted co-pyrolysis of TS with auxiliary organic residues like furfural residue dramatically boosts heating uniformity and devolatilization efficiency, resulting in higher bio-oil yields and significantly reduced

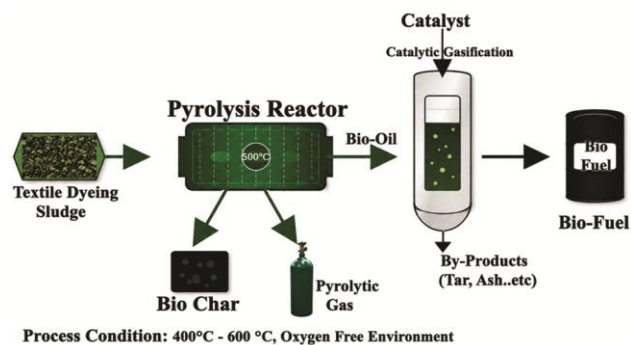


Fig. 8 — Schematics of the pyrolysis process

nitrogen and sulfur-containing compounds. This method improves the oil quality, but its success hinges on the availability of suitable co-feedstocks and largely remains constrained to laboratory-scale systems due to microwave penetration limits and energy demands<sup>20,21</sup>.

Microwave-assisted auger pyrolysis facilitates continuous operation with exceptional energy and exergy efficiencies under optimized conditions. Despite its immense potential for process intensification, reactor complexity, capital costs, and limitations in treating high ash or salt-loaded TS restrict its practical application on an industrial scale<sup>22</sup>. Thermo-catalytic pyrolysis employing mineral or synthetic catalysts (e.g., kaolin, zeolites) significantly enhances volatile release, improves oil quality, and fosters the immobilization of heavy metals within biochar. However, catalyst fouling caused by inorganic ash and alkali salts remains a significant operational challenge for processing TS<sup>23,24</sup>.

### Environmental Impacts of Pyrolysis

Pyrolysis of TS has enormous environmental benefits by significantly lowering Green House Gas (GHG) emissions compared to landfilling and incineration, while facilitating carbon sequestration through biochar and renewable fuel substitution through bio-oil<sup>25,26</sup>. Heavy metals are contained within the char matrix, lowering leachability and environmental threats, especially when potent additives are used<sup>27,28</sup>. Nonetheless, salt-induced corrosion and ash-related fouling continue to challenge long-term reactor stability and product purity<sup>29-31</sup>. Pyrolysis is extremely suitable for bio-sludge TS due to its high organic and volatile content, conditionally feasible for salt-sludge with significant material and corrosion constraints, and entirely unsuitable for Lime-sludge due to its predominantly inorganic composition and minimal energy yield. The comparative environmental and economic implications of different pyrolysis routes are summarized in Table 3.

### Torrefaction

Torrefaction is an essential mild thermochemical pretreatment (200-300°C, oxygen-limited) that demands attention for managing TS due to its undeniable capability to convert organic fractions into a stable, carbon-rich biochar while effectively minimizing gaseous emissions. When we look at high-temperature processes, torrefaction stands out by prioritizing the stabilization of materials and resource recovery over direct energy production, which is crucial for sludge streams rich in organic materials. A schematic representation of the torrefaction process is shown in Fig. 9. During torrefaction, the organic matter of TS undergoes partial thermal decomposition and carbonization, resulting in a reduction of volatile matter and a significant increase in fixed carbon content, thereby substantially enhancing biochar stability and heavy-metal immobilization<sup>32</sup>. Concurrently, surface functional groups are systematically restructured, leading to the formation of oxygen-containing functionalities (-OH, C-O),

Table 3 — Comparison of different Pyrolysis methods

Technique	Process Parameters	Environmental Benefits	TS Suitability & Constraints	Ref.
Microwave Co-Pyrolysis	400–600°C, Microwave heating, Inert atmosphere	Reduces nitrogen and sulfur; yields high-quality bio-oil	Bio-sludge is suitable; Salt sludge degrades oil; Lime-sludge is ineffective	[20,21]
Catalytic Pyrolysis	450–650°C, Catalysts (Zeolite, Ni, Fe), Inert gas	Enhances bio-oil yield and quality; stabilizes heavy metals	Bio-sludge is effective; salt/ash foul catalysts; Lime-sludge is inactive	[58,59]
Co-Pyrolysis with Waste	400–700°C, Mixed feedstocks, Inert or oxidative	Transforms hazardous waste into valuable chemicals and fuels	Bio-sludge conditional; feed variability limits control	[18,58]
Microwave-Assisted Auger Pyrolysis	450–600°C, Continuous auger system, Microwave heating	Achieves high energy and exergy efficiencies	Bio-sludge applicable; scale-up limited	[22]
Thermo-Catalytic Pyrolysis	500–700°C, Catalysts (Metal oxides, Zeolites),	Improves product yields and quality; reduces environmental risks	Bio-sludge favoured; ash deactivates catalysts	[25,28]

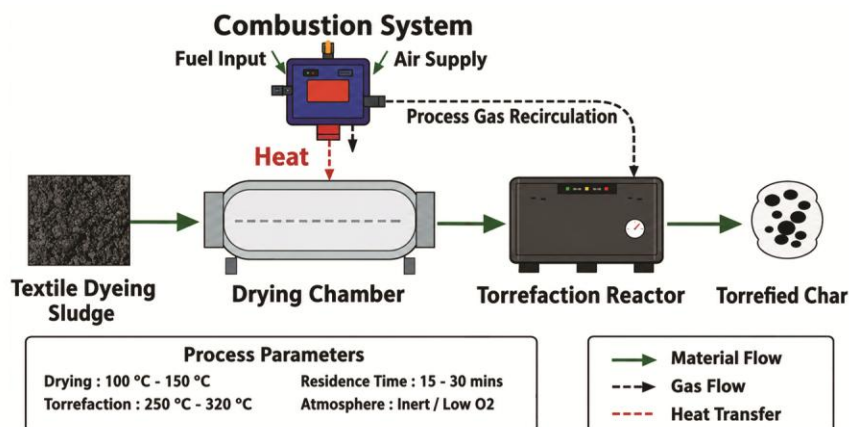


Fig. 9 — Schematics of the torrefaction process

which drastically improve adsorption affinity toward dyes and dissolved pollutants<sup>33</sup>. Structural rearrangement also increases surface area and pore volume; for instance, ZnCl<sub>2</sub>-modified TS biochar achieved an impressive surface area of 495.38 m<sup>2</sup> g<sup>-1</sup>, facilitating efficient adsorption of Malachite Green (MG)<sup>34</sup>. These combined physicochemical shifts decisively frame torrefaction as a crucial initial phase for upcoming adsorption, fuel refinement, or soil applications, rather than being merely a standalone breakdown method.

#### Advantages of torrefaction

Torrefaction of TS delivers substantial environmental and functional benefits while operating at comparatively low temperatures (200–300°C). Heavy metal bioavailability is reduced through mineral stabilization, with co-torrefaction utilizing CaO or modified kaolin reducing the ecological Risk Index (RI) from 154.45 (raw TS) to 11.18, achieving an over 90% risk reduction<sup>33,35</sup>. The process of biochar formation stabilizes carbon and can lead to GHG emission reductions up to 57.4% when compared to coal burning, particularly when torrefied biochar acts as a substitute fuel.

Simultaneously, surface functionalization and pore development significantly enhance adsorption performance; TS-derived biochar achieved an exceptional >99% dye removal efficiency for Malachite Green and azo dyes, with adsorption capacities soaring to 224.1 mg g<sup>-1</sup> (Ref.<sup>36,37</sup>). When combined with lignocellulosic residues, torrefaction also markedly improves fuel quality, producing biochar with a Higher Heating Value (HHV) of up to 23.62 MJ kg<sup>-1</sup>, enabling effective downstream gasification or co-combustion applications<sup>38</sup>. These quantified advantages firmly establish torrefaction as a material stabilization and valorization route, rather than a mere primary energy recovery technology.

#### Environmental benefits of torrefaction

Torrefaction plays a pivotal role in sustainable TS management by significantly reducing landfill dependency, immobilizing hazardous constituents, and generating high-value biochar products. Blending TS with lignocellulosic residues such as bamboo or sugarcane bagasse further amplifies energy and exergy efficiencies, yielding biochar with HHV values reaching 23.62 MJ kg<sup>-1</sup>, perfectly suitable for gasification or co-combustion applications<sup>33,39,40</sup>. As an adsorbent or a soil amendment, torrefied biochar significantly contributes to addressing waste disposal, cleaning pollutants, and reducing the carbon footprint<sup>32,39</sup>.

Table 4 lays out a comprehensive comparison of multiple torrefaction strategies, detailing their operational features and efficiency results, skillfully revealing the subtle interplay between environmental safeguarding and energy retrieval. While torrefaction efficiently stabilizes heavy metals and generates functional biochar from bio-sludge, its limited energy recovery, sensitivity to salt-rich TS, and application-specific economic viability hinder large-scale adoption in comparison to pyrolysis and incineration.

#### Hydrothermal Processes

Hydrothermal processing encompasses Hydrothermal Liquefaction (HTL) and Hydrothermal Carbonization (HTC), both of which exploit subcritical water to treat wet TS without energy-intensive drying, directly aligning with the high moisture content and organic variability identified in the characterization section. These routes differ in severity and product focus but share common advantages for sludge stabilization and resource recovery (Figs. 10a and 10b). The organic-rich bio-sludge, characterized by elevated carbon and hydrogen content, responds favourably to both HTL

Table 4 — Comparison of Torrefaction conditions and outcomes

Method of torrefaction	Parameter	Key findings	Outcome	Ref.
Co-pyrolysis torrefaction	300–600°C, Co-pyrolysis with CaO	Co-pyrolysis with CaO increased stable heavy metal fractions by 75%–100%.	Heavy metal immobilization	[34]
Hydrothermal Torrefaction	400–600°C, Activated biochar, pH control	Biochar achieved 99.13% MG removal at optimal conditions.	Dye removal capacity	[37]
Conventional torrefaction	250–350°C, Blended sludge & bagasse	Torrefaction of blended sludge and bagasse achieved HHV up to 23.62 MJ/kg.	Energy yield	[39]
Microwave-assisted torrefaction	450°C, Sludge and furfural feedstocks	Energy and exergy efficiencies optimized at 450°C for sludge and furfural.	GHG mitigation	[33]
Conventional torrefaction	250–350°C, Biomass conversion	Biochar production reduced GHG emissions by 57.4% compared to coal burning.	Resource recovery	[40]

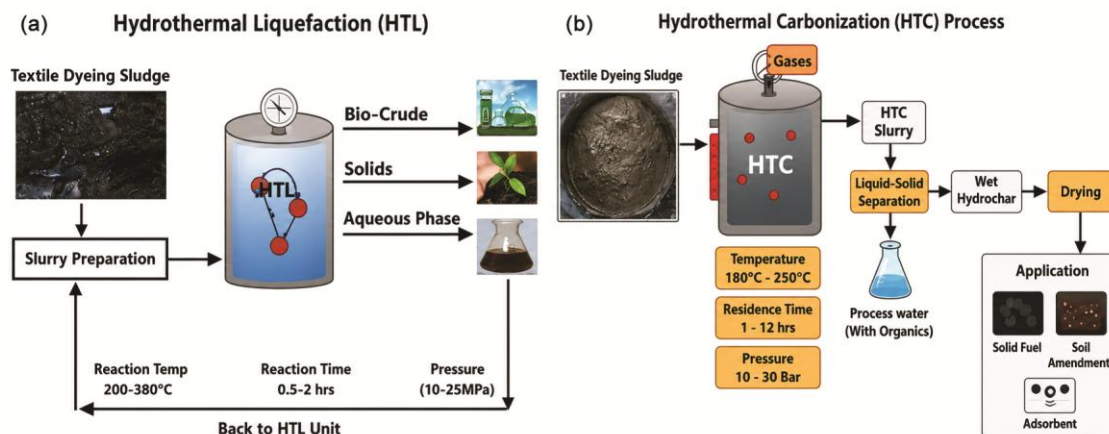


Fig. 10 — Schematic representation of the (a) HTL process flow and (b) HTC remediation of TS

Table 5 — Comparative analysis of HTL Studies

Type of HTL	Operating parameters	Key findings	Ref.
Catalytic HTL	350°C, 30min, KOH catalyst	58wt% bio-oil yield, 94% energy recovery	[42]
Co-HTL	325°C, 95% Cotton/5% PET mix	26% bio-oil yield, 48-91% TPA yield	[43]
Waste Biomass HTL	350°C, 10 min, Municipal sludge	42.5% bio-oil yield, higher compound diversity	[54]
Co-Liquefaction HTL	350°C, 15 min, Sewage sludge	12.0% biocrude yield, co-liquefaction effects	[49]
Catalytic HTL	350°C, 30 min, Various catalysts	Enhanced bio-oil quality with Ni@CSB catalyst	[53]

and HTC, yielding energy-dense bio-oil (up to 58 wt%) under HTL<sup>41-44</sup> and stable hydrochar with energy recovery up to 82.44% under HTC<sup>45</sup>. In contrast, salt-sludge, identified by high conductivity and sodium content, limits process efficiency through bio-crude contamination and catalyst deactivation, while lime-sludge, dominated by inorganic CaCO<sub>3</sub> phases, lacks suitable precursors for either bio-oil or hydrochar formation.

#### Advantages and Limitations

Hydrothermal routes achieve up to 94% energy recovery (HTL)<sup>41</sup> and sludge volume reduction up to 90% (HTC)<sup>46</sup>, while significantly lowering GHG emissions relative to incineration and landfilling (up to 98%)<sup>47-50</sup>. Heavy metals are immobilized within hydrochar or biochar matrices, thereby significantly reducing leachability to mitigate environmental risk<sup>45,46,50,51</sup>. Process performance is extremely sensitive to feedstock composition, with excessive salts promoting catalyst fouling (HTL) and inhibiting hydrochar quality (HTC). Higher temperatures increase PAH formation in HTL<sup>52</sup>, while extended reaction times in HTC raise energy demand and reduce net efficiency, as tabulated in Table 5.

#### Constraints for TS

For bio-sludge, hydrothermal processing is highly effective, can be conditionally applied to salt-sludge,

but is outright unsuitable for lime-sludge. Despite their advantages for wet biomass, hydrothermal routes are only partially suitable for TS due to its distinct physicochemical characteristics. TS typically contains high concentrations of inorganic salts (Na<sup>+</sup>, Cl<sup>-</sup>, SO<sub>4</sub><sup>2-</sup>), residual dyes and auxiliary chemicals, which promote bio-crude contamination, catalyst deactivation and phase instability during HTL<sup>43,52-54</sup>. The low lipid fraction of TS further restricts bio-oil yield compared to sewage or algal sludges, limiting fuel quality enhancement<sup>41,42</sup>. In HTC, increased ash and salt contents hinder carbon densification and reduce hydrochar yield, while increasing the salinity of process water and downstream treatment demand<sup>50,51</sup>. Additionally, lime-rich TS, dominated by CaCO<sub>3</sub> as confirmed by PXRD and TGA, lacks thermochemically reactive organic precursors, rendering both HTL and HTC technically inefficient for energy recovery. Consequently, hydrothermal processing of TS is best suited as a stabilization and volume-reduction strategy rather than a primary fuel-generation pathway. Table 6 summarizes HTL operating conditions and yields, while Table 6 outlines HTC parameter effects on hydrochar properties.

#### Challenges and Future Research

##### Technological constraints

The treatment of TS is fundamentally constrained by its high salinity, complex dye chemistry,

Table 6 — Effects of different parameters on hydrochar from the HTC process

Parameter	Effect on hydrochar properties	Ref.
Temperature (180-300 °c)	Reduces H/C and O/C ratios, increases energy density	[45,51]
Pressure (6.1-34.2 kg/cm <sup>2</sup> )	Enhances dehydration and decarboxylation reactions	[50]
Reaction time (30min – 5hrs)	Increase carbon content, reduces volatile matter	[45,51]

Table 7 — Cost and feasibility comparison of TS treatment and valorization routes

\*TRL: Technology Readiness Level (1 = laboratory, 9 = commercial)

Technology	TRL*	Energy demand	Environmental risk	Industrial feasibility	Technology sensitivity to TS type
<i>Biological Treatment</i>	7–9	Low	Medium	Limited	Bio: Effective Salt: Inhibited Lime: Ineffective
<i>Enzymatic Processes</i>	2–3	Low	Low	Poor	Bio: Selective; Salt: Deactivated; Lime: Inactive
<i>Membrane Processes (MBR, NF/RO)</i>	6–8	Medium–high	Medium	Moderate	Bio: Treatable; Salt: Fouling; Lime: Scaling
<i>Hydrothermal Carbonization (HTC)</i>	4–6	Medium	Low	Emerging	Bio: Suitable; Salt: Corrosion; Lime: Non-reactive
<i>Hydrothermal Liquefaction (HTL)</i>	3–5	High	Medium	Low	Bio: Favorable; Salt: Bio-oilcontamination. Lime: Unsuitable
<i>Incineration /Combustion</i>	8–9	Very high	High	High	Bio: Effective. Salt: Lime recovery
<i>Pyrolysis</i>	5–7	High	Low–medium	Moderate	Bio: Optimal; Salt: Char contamination; Lime: Ineffective
<i>Co-pyrolysis / Integrated Thermochemical thermochemical</i>	6–8	Medium	Low	High	Bio: Optimal; Salt: Diluted effects; Lime: Stabilizer
<i>Simulation-assisted Integrated pyrolysis</i>	3–5	Medium	Low	Emerging	Bio: Scalable; Salt: Manageable. Lime: Auxiliary

heterogeneous organic or inorganic composition, and heavy metal content, which limit the effectiveness and scalability of both conventional and advanced remediation technologies. Biological processes are severely inhibited by azo dyes and elevated salt concentrations, which induce osmotic stress and suppress microbial activity, rendering them unsuitable as standalone solutions. The processes of pyrolysis and gasification within thermochemical pathways encounter significant obstacles from high moisture content, inorganic salts, and ash, causing an escalation in energy needs, corrosion of reactors, formation of slag, and a clear drop in product quality. The sensitivity of torrefaction to changes in feedstock is pronounced, leading to its restriction to bio-sludge because of poor tolerance for inorganic fractions. Hydrothermal approaches tackle moisture-related limitations to a certain extent but are still affected by salt, synthetic fibres, and components that do not hydrolyze, which can significantly undermine the quality of bio-oil or hydrochar and complicate downstream applications. Although incineration is a technique that holds wide acceptance, it encounters

several issues, including ineffective combustion performance, substantial emissions, and the complex management of ash that contains salt when applied to TS. To convert sludge characterization into decisive technology choices, Table 7 compares key remediation and valorization pathways regarding techno-economic performance, sustainability, and their distinct reactions to bio, salt, and lime sludge, synthesized from published literature and technology readiness assessments.

#### Economical constraint

Economic feasibility is an unyielding barrier for TS remediation due to high capital intensity, elevated energy demand, and additional downstream treatment requirements across most technology classes. Although biological treatments have low capital costs, extended retention times and process instability increase operational expenses. Engaging in thermochemical techniques like pyrolysis, gasification, HTL, and HTC entails a major financial outlay for reactors operating at high temperatures or pressures, in conjunction with costs linked to drying, upgrading, catalyst substitution, and managing

Table 8 — Cost and feasibility comparison of TS treatment and valorization routes

Technology	Capital intensity	Operating cost	Energy efficiency	Cost drivers	Economic viability for TS
Biological treatment	Low	Medium	Low–medium	Long HRT, monitoring	Limited (salt inhibition)
Enzymatic processes	Low	Very high	High	Enzyme replacement	Poor
Membrane systems	High	High	Low	Fouling, cleaning	Limited
Torrefaction	Medium	Low–medium	Medium	Drying, feed variability	Bio-sludge only
Pyrolysis	High	High	Medium	Drying, heating,	Good
Co-pyrolysis	Medium–high	Medium	High	Feed blending	Good
HTC	High	Medium	Medium	Pressure systems	Moderate
HTL	Very high	Very high	High	Pressure, catalysts	Low
Incineration	Very high	Very high	Low	Emission control	Regulatory driven
Integrated thermochemical	Medium–high	Medium	High	System integration	Most promising

emissions. While torrefaction has the benefit of lower capital costs, it is critically constrained by limited market demand and varying product quality. Incineration results in significant energy challenges due to sludge moisture and the stringent regulatory compliance costs. Table 8 provides a qualitative, decision-oriented comparison of the key economic constraints associated with major treatment and valorization technologies for TS, integrating capital intensity, operating costs, energy efficiency, and dominant cost drivers reported in the literature.

#### Environmental constraint

Environmental concerns associated with TS treatment are principally linked to secondary pollution, toxic by-product formation, and residue management. Biological processes may leave residual dyes and metals, generating excessive secondary sludge. Pyrolysis, gasification, and torrefaction can emit VOCs, PAHs, and GHGs if not controlled, while residual char or ash may retain immobilized heavy metals requiring regulated disposal. Hydrothermal processes generate aqueous effluents enriched with organic acids, salts, and metals, demanding advanced wastewater treatment. Incineration poses the highest environmental risk among the evaluated technologies due to dioxin formation, metal volatilization, and hazardous ash generation.

#### Regulatory constraints

Regulatory constraints hinder the widespread adoption of TS treatment technologies in the Indian textile sector. Compliance with emission and disposal standards set by the Central Pollution Control Board (CPCB), including strict limits on dioxins, particulate matter, NO<sub>x</sub>, SO<sub>2</sub>, and heavy-metal leachability, demands rigorous operational and monitoring

protocols for thermochemical processes. Furthermore, the absence of clear CPCB guidelines for the reuse of sludge-derived char, ash, or construction materials, along with inconsistent regional regulatory enforcement, generates significant approval uncertainty and impedes industrial-scale implementation even when technical feasibility is already established.

#### Logistical and scale-up barriers

Large-scale implementation of TS remediation technologies is undeniably limited by pretreatment requirements, feedstock heterogeneity, infrastructure compatibility, and operational complexity. Most technologies demand extensive preprocessing, such as dewatering, drying, homogenization, or size reduction, which significantly increases logistical burden and cost. The transportation of high-moisture sludge further constrains scalability. Hydrothermal and incineration systems require specialized infrastructure and skilled operation, which are often absent in textile treatment facilities. Maintaining consistent feedstock quality is an unmistakable bottleneck for continuous operation.

#### Research gaps and future directions in sludge remediation

- Pretreatment: Develop advanced pretreatment to remove salt, microplastics, and heavy metals while reducing by-product toxicity.
- Hybrid systems: Explore integrated biological, thermochemical, and physicochemical pathways to enhance resource recovery.
- Construction use: Standardize TS characterization, optimize replacement ratios, and assess long-term durability and regulation.
- Sustainability: Apply LCA and techno-economic analysis to benchmark energy, cost, and environmental trade-offs.

## Conclusion

This review conclusively evaluates remediation, valorization, and reuse strategies for TS, clearly differentiating bio-sludge, salt-sludge, and lime-sludge, as their distinct organic composition, ash content, salinity, and calcium prevalence critically influence technology performance. Pyrolysis and HTC are the most effective methods for bio-sludge due to its elevated volatile matter and fixed carbon levels, facilitating significant volume reduction and energy recovery. HTL can efficiently process high-moisture TS, but factors including corrosion from salt, catalyst impairment, and costly operations restrict its genuine potential. Salt-sludge, with its high ionic strength and residual dye salts, obstructs biological processes through osmotic stress and severely undermines catalytic and membrane-based systems due to fouling. Conversely, lime-sludge, primarily composed of inorganic calcium phases, is entirely unsuitable for biochemical or thermochemical conversion; however, it excels in incineration and construction material applications because of its mineral reactivity and stabilization capabilities. Incineration and co-combustion demonstrate the highest level of technological maturity (TRL 8–9) but confront stringent emission regulations and ash management challenges, specifically under CPCB regulations relevant to the Indian textile sectors. Innovative integrated and simulation-assisted thermochemical systems are set to enhance energy efficiency and process control; nonetheless, pilot-scale validation using actual TS feedstocks is still inadequate. Ultimately, energy demands, pre-processing intensity, emission control obligations, and regulatory compliance dictate feasibility, establishing hybrid treatment frameworks as the optimal route for sustainable TS management. By aligning sludge properties with technology readiness, regulatory compliance, and resource recovery potential, TS can be transformed from a disposal burden into a circular resource stream supporting SDGs 6 (Clean Water), 7 (Clean Energy), 9 (Industry & Innovation), 12 (Responsible Consumption), and 13 (Climate Action).

## Conflict of Interest

The authors declare that they have no competing interests.

## Acknowledgements

The authors are thankful to Mrs. Rukmani Subramanian for the funding provided for the characterisation of the samples. The authors would like to express their gratitude to the Sophisticated Test

and Instrumentation Centre (STIC), Cochin University of Science and Technology (CUSAT), for characterisation of the samples.

## References

- 1 Agarwal R, Golden era of Indian textile industry, *Int J Trend Sci Res Dev*, 3 (2019).
- 2 Tandon N & Reddy E, A study on emerging trends in textile industry in India, *Int J Adv Res Technol*, 2 (2013).
- 3 Nelliya P, A case study of tiruppur textile cluster, (2007).
- 4 TNPCB, Details of common effluent treatment plants pertaining to the cluster of tannery industries in Tamil Nadu, (2022) 9.
- 5 Ghumra D P, Agarkoti C & Gogate P R, Improvements in effluent treatment technologies in common effluent treatment plants (CETPs): Review and recent advances, *Process Saf Environ Prot*, 147 (2021) 1018.
- 6 Raju L & Kumar D V, Biological sludge from textile dyeing effluent treatment plant- characterization, combustion simulation and its impact on air pollution, *Results Eng*, 25 (2025) 103850.
- 7 Nancharaiyah Y V & Reddy G K K, Aerobic granular sludge technology: Mechanisms of granulation and biotechnological applications, *Bioresour Technol*, 247 (2018) 1128.
- 8 Upadhyay R, Khan H I U H & Przystaś W, An evaluation of decolorization mechanism of synthetic dyes belonging to the azo, anthraquinone, and triphenylmethane group, as a sustainable approach, by immobilized CB8 strain (*Trametes versicolor*), *Desal Water Treat*, 284 (2023) 268.
- 9 Xie C, Liu J, Xie W, Kuo J, Lu X, Zhang X, He Y, Sun J, Chang K, Xie W, Liu C, Sun S, Buyukada M & Evrendilek F, Quantifying thermal decomposition regimes of textile dyeing sludge, pomelo peel, and their blends, *Renew Energy*, 122 (2018) 55.
- 10 Jeevanandam S, Ravikumar K, Das A & Goel M, Comprehensive study on textile dyeing sludge as a substitute for cement in cement-mortar, *Int J Technol*, 5 (2015) 219.
- 11 Lin M, Ning X A, Liang X, Wei P, Wang Y & Liu J, Study of the heavy metals residual in the incineration slag of textile dyeing sludge, *J Taiwan Inst Chem Eng*, 45 (2014) 1814.
- 12 Vasques M A R, Selene S M A, Valle J A B & De-Souza A A U, Thermogravimetric analysis and kinetic study of pyrolysis and combustion of residual textile sludge, *J Therm Anal Calorim*, 121 (2015) 807.
- 13 Liu Y, Ran C, Siddiqui A R, Mao X, Kang Q, Fu J, Deng Z, Song Y, Jiang Z, Zhang T, Ao W & Dai J, Pyrolysis of textile dyeing sludge in fluidized bed: Characterization and analysis of pyrolysis products, *Energy*, 165 (2018) 720.
- 14 Feodorov V, Modern technologies of treatment and stabilization for sewage sludge from water treatment plant, *Agric Agric Sci Procedia*, 10 (2016) 417.
- 15 Canabarro N, Soares J F, Anchieta C G, Kelling C S & Mazutti M A, Thermochemical processes for biofuels production from biomass, 1 (2013) 22.
- 16 Cengiz N Ü, Yildirim E, Sağlam M, Yüksel M & Ballice L, Hydrogen and methane production from tomato processing plant waste by hydrothermal gasification, *J Supercrit Fluids*, 190 (2022) 105751.
- 17 Yildirim E & Ballice L, Supercritical water gasification of wet sludge from biological treatment of textile and leather industrial wastewater, *J Supercrit Fluids*, 146 (2019) 100.

- 18 Zhang S, Xu Y, Bie X, Li Q, Zhang Y & Zhou H, Mechanisms in CO<sub>2</sub> gasification and co-gasification of combustible solid waste: A critical review, *Gas Sci Eng*, (2024) 205368.
- 19 Liu Y, Ran C, Siddiqui A R, Mao X, Kang Q, Fu J, Deng Z, Song Y, Jiang Z, Zhang T & Dai J, Pyrolysis of textile dyeing sludge in fluidized bed and microwave-assisted auger reactor: Comparison and characterization of pyrolysis products, *J Hazard Mater*, 359 (2018) 454.
- 20 dos Santos J M, Zelioli Í A M & Mariano A P, Hybrid modeling of machine learning and phenomenological model for predicting the biomass gasification process in supercritical water for hydrogen production, *Engineering*, 4 (2023) 1495.
- 21 Wu L, Guan Y, Li C, Shi L, Yang S, Reddy B R, Ye G, Zhang Q, Liew R K & Zhou J, Free-radical behaviors of co-pyrolysis of low-rank coal and different solid hydrogen-rich donors: A critical review, *Chem Eng J*, 474 (2023) 145900.
- 22 Ran C, Liu Y, Siddiqui A R, Siyal A A, Mao X, Kang Q, Fu J, Ao W & Dai J, Pyrolysis of textile dyeing sludge in fluidized bed and microwave-assisted auger reactor: Comparison, migration and distribution of heavy metals, *Energy*, 182 (2019) 337.
- 23 Zhang H, Gao Z, Liu Y, Ran C, Mao X, Kang Q, Ao W, Fu J, Li J, Liu G & Dai J, Microwave-assisted pyrolysis of textile dyeing sludge, and migration and distribution of heavy metals, *J Hazard Mater*, 355 (2018) 128.
- 24 Li C, Zhang J, Shan R, Yuan H & Chen Y, Kinetic study for thermocatalytic degradation of waste mixed cloth over antibiotic residue derived carbon-based solid acids, *Fuel*, 331 (2023) 125797.
- 25 Csutoras B & Miskolczi N, Thermo-catalytic pyrolysis of sewage sludge and techno-economic analysis: The effect of synthetic zeolites and natural sourced catalysts, *Bioresour Technol*, 400 (2024) 130676.
- 26 Gong B, Tian C, Wang X, Chen X & Zhang J, Mineralogical characteristics and arsenic release of high arsenic coals from southwestern guizhou, china during pyrolysis process, *Processes*, 11 (2023) 2321
- 27 Zaharioiu A M, Niculescu V C, Sandru C, Spiridon S I, Soare A, Oancea S & Marin F, The valorisation of biochar produced from black liquor pyrolysis for the development of CO<sub>2</sub> adsorbents, *Molecules*, 29 (2024) 5613.
- 28 Li J, Xu K, Yao X & Liu J, Investigation of biomass slow pyrolysis mechanisms based on the generation trends in pyrolysis products, *Process Saf Environ Prot*, 183 (2024) 327.
- 29 Barry D, Barbiero C, Briens C & Berruti F, Pyrolysis as an economical and ecological treatment option for municipal sewage sludge, *Biomass Bioenergy*, 122 (2019) 472.
- 30 Kiran S, Ghaffar A, Iqbal S, Javed S, Aslam N, Rafique M A, Zreen Z, Afzal G, Parveen N & Naz S, Characterization and valorization of sludge from textile wastewater plant for positive environmental applications, *Handbook Biomass Valor Ind Appl*, (2022) 465–489
- 31 Agar D A, Kwapinska M & Leahy J J, Pyrolysis of wastewater sludge and composted organic fines from municipal solid waste: laboratory reactor characterisation and product distribution, *Environ Sci Pollut Res*, 25 (2018) 35874.
- 32 He H, Lu S, Peng Y, Tang M, Zhan M, Lu S, Xu L, Zhong W & Xu L, Emission characteristics of dioxins during iron ore Co-sintering with municipal solid waste incinerator fly ash in a sintering pot, *Chemosphere*, 287 (2022) 131884.
- 33 Rago Y P, Surroop D & Mohee R, Torrefaction of textile waste for production of energy-dense biochar using mass loss as a synthetic indicator, *J Environ Chem Eng*, 6 (2018) 811.
- 34 Lin S L, Zhang H, Chen W H, Song M & Kwon E E, Low-temperature biochar production from torrefaction for wastewater treatment: A review, *Bioresour Technol*, 387 (2023) 129588.
- 35 Liu Q, Zheng H, Zhang P, Guo X, Deng W, Xu K, Xu J, Jiang L, Wang Y & Xiang J, Enhancing pyrolysis of automobile shredder residue through torrefaction: Interactions among typical components, *Fuel*, 390 (2025) 134670.
- 36 Hu J, Song Y, Liu J, Evrendilek F, Buyukada M & Yan Y, Synergistic effects, gaseous products, and evolutions of NO<sub>x</sub> precursors during (co-)pyrolysis of textile dyeing sludge and bamboo residues, *J Hazard Mater*, 401 (2021) 123331.
- 37 Qian L, Mei C, Li T, Luo W, Liu W, Chen M, Yang X, Li X, Cheng B & Ma H, A versatile biochar fertilizer used for adsorption of heavy metals and enhancement of plant growth in metal contaminated soil, *Environ Technol Innov*, 36 (2024) 103743.
- 38 Ravindiran G, Sundaram H, Rajendran E M, Ramasamy S, Nabil A Z & Ahmed B, Removal of azo dyes from synthetic wastewater using biochar derived from sewage sludge to prevent groundwater contamination, *Urban Clim*, 49 (2023) 101502.
- 39 Nwabunwanne N, Vuyokazi T, Olagoke A, Mike O, Patrick M & Anthony O, Torrefaction characteristics of blended ratio of sewage sludge and sugarcane bagasse for energy production, *Appl Sci*, 11 (2021) 2654.
- 40 Lin Y L, Zheng N Y & Wang H C, Sludge dewatering through H<sub>2</sub>O<sub>2</sub> lysis and ultrasonication and recycle for energy by torrefaction to achieve zero waste: An environmental and economical friendly technology, *Renew Sustain Energy Rev*, 155 (2022) 111857.
- 41 Chang Y C, Xiao X F, Huang H J, Xiao Y D, Fang H S, He J B & Zhou C H, Transformation characteristics of polycyclic aromatic hydrocarbons during hydrothermal liquefaction of sewage sludge, *J Supercrit Fluids*, 170 (2021) 105158.
- 42 Hegdahl S H, Løhre C & Barth T, Hydrothermal liquefaction of sewage sludge anaerobic digestate for bio-oil production: Screening the effects of temperature, residence time and KOH catalyst, *Waste Manag Res*, 41 (2023) 977.
- 43 Matayeva A & Biller P, Hydrothermal liquefaction of post-consumer mixed textile waste for recovery of bio-oil and terephthalic acid, *Resour Conserv Recycl*, 185 (2022) 106502.
- 44 Govindasamy G & Kumar J P, Hydrothermal liquefaction of food waste to bio-oil over hierarchical Fe-Co-ZSM-5 catalyst for the circular economy, *Mater Today Proc*, 65 (2022) 3688.
- 45 Hejna M, Świechowski K & Białowiec A, Study on the effect of hydrothermal carbonization parameters on fuel properties of sewage sludge hydrochar, *Materials*, 16 (2023) 6903.
- 46 Mannarino G, Sarrion A, Diaz E, Gori R, De la Rubia M A & Mohedano A F, Improved energy recovery from food waste through hydrothermal carbonization and anaerobic digestion, *Waste Manag*, 142 (2022) 9.

- 47 Strugała-Wilczek A, Basa W, Pankiewicz-Sperka M, Xu D, Duan P, Hao B, Wang Y, Leng L, Yang L & Fan L, Distribution characteristics and migration pathways of metals during hydrothermal liquefaction of municipal sewage sludge in the presence of various catalysts, *Sci Total Environ*, 920 (2024) 171023.
- 48 Un C, Enhancing sewage sludge treatment with hydrothermal processing: A case study of adana city, *Sustainability*, 16 (2024) 4174.
- 49 Ellersdorfer M, Hydrothermal co-liquefaction of chlorella vulgaris with food processing residues, green waste and sewage sludge, *Biomass Bioenergy*, 142 (2020) 105796.
- 50 Malhotra M & Garg A, Hydrothermal carbonization of sewage sludge: Optimization of operating conditions using design of experiment approach and evaluation of resource recovery potential, *J Environ Chem Eng*, 11 (2023) 109507.
- 51 Rathika K, Kumar S & Yadav B R, From pollutant to powerhouse: The untapped potential of sewage sludge and wastewater, *EMBO Rep*, 24 (2023) e58201.
- 52 Sharma P, Sharma S, Sharma S K, Jain A & Shrivastava K, Review on recent advancement of adsorption potential of sugarcane bagasse biochar in wastewater treatment, *Chem Eng Res Des*, 206 (2024) 428.
- 53 Le T H, Wang S, Kim B S, Nam H & Lee D, Advancements and challenges in catalytic hydrothermal liquefaction of lignocellulosic biomass: A comprehensive review, *Chem Eng J*, 498 (2024) 155559.
- 54 Di-Lauro F, Amadei A, Balsamo M, Damizia M, de-Capraia B, De-Filippis P, Solimene R, Salatino P & Montagnaro F, Effect of the reactor heating rate on bio-crude yield and quality from hydrothermal liquefaction of different sludge, *Fuel Commun*, 19 (2024) 100113.
- 55 Zhang W, Chen J, Fang H, Zhang G, Zhu Z, Xu W, Mu L & Zhu Y, Simulation on co-gasification of bituminous coal and industrial sludge in a downdraft fixed bed gasifier coupling with sensible heat recovery, and potential application in sludge-to-energy, *Energy*, 243 (2022) 123052.
- 56 Lin D, Kai W, Xie X, Kozlov A, Penzik M & Li B, Steam gasification of lime dried sewage sludge: Effects of temperature and addition of lime, *Fuel*, 371 (2024) 131932.
- 57 Lan W, Chen G, Zhu X, Wang X, Liu C & Xu B, Biomass gasification-gas turbine combustion for power generation system model based on ASPEN PLUS, *Sci Total Environ*, 628 (2018) 1278.
- 58 Lin L, Yang E, Sun Q, Chen Y, Dai W, Bao Z, Niu W & Meng J, Analysis of the pyrolysis kinetics, reaction mechanisms, and by-products of rice husk and rice straw via TG-FTIR and Py-GC/MS, *Molecules*, 30 (2024) 10.
- 59 Zhang X, Zhao B, Liu H, Zhao Y & Li L, Effects of pyrolysis temperature on biochar's characteristics and speciation and environmental risks of heavy metals in sewage sludge biochars, *Environ Technol Innov*, 26 (2022) 102288.